Key Points:
- Unprecedented dry soil contributed to the 2018 European heatwave and drought by altering surface fluxes, heating, and drying the atmosphere
- Threshold values of soil water content are found below which air temperature becomes much more sensitive to increased drying
- Field observations corroborate reanalysis depictions of heatwave sensitivity, suggesting land feedbacks amplified heat over much of Europe

Correspondence to:
P. A. Dirmeyer,
pdirmeye@gmu.edu

Author Contributions:
Conceptualization: Paul A. Dirmeyer, Gianpaolo Balsamo
Data curation: Eleanor M. Blyth, Ross Morrison

Land-Atmosphere Interactions Exacerbated the Drought and Heatwave Over Northern Europe During Summer 2018

Paul A. Dirmeyer[1] [iD], Gianpaolo Balsamo[2] [iD], Eleanor M. Blyth[3], Ross Morrison[3] [iD], and Hollie M. Cooper[3] [iD]

[1]Center for Ocean-Land-Atmosphere Studies, George Mason University, Fairfax, VA, USA, [2]European Centre for Medium-range Weather Forecasts, Reading, UK, [3]UK Centre for Ecology and Hydrology, Wallingford, UK

Abstract The 2018 drought and heatwave over northern Europe were exceptional, with unprecedented forest fires in Sweden, searing heat in Germany and water restrictions in England. Monthly, daily, and hourly data from ERA5, verified with in situ soil water content and surface flux measurements, are examined to investigate the subseasonal-to-seasonal progression of the event and the diurnal evolution of tropospheric profiles over Britain to quantify the anomalous land surface contribution to heat and drought. Data suggest the region entered an unprecedented condition of becoming a "hot spot" for land-atmosphere coupling, which exacerbated the heatwave across much of northern Europe. Land-atmosphere feedbacks were prompted by unusually low soil water over wide areas, which generated moisture limitations on surface latent heat fluxes, suppressing cloud formation, increasing surface net radiation, and driving temperatures higher during several multiweek episodes of extreme heat. We find consistent evidence in field data and reanalysis of a threshold of soil water content at most locations, below which surface fluxes and daily maximum temperatures become hypersensitive to declining soil water. Similar recent heatwaves over various parts of Europe in 2003, 2010, and 2019, combined with dire climate change projections, suggest such events could be on the increase. Land-atmosphere feedbacks may play an increasingly important role in exacerbating extremes, but could also contribute to their predictability on subseasonal time scales.

Plain Language Summary This study uses a combination of environmental observations, atmospheric, and land surface analyses over northern Europe to examine the exceptional drought and heatwave during the summer of 2018. Results suggest the region entered a state of positive feedback between the land and atmosphere, exacerbating the heatwave over the area. This is a situation that is common over southern Europe and many other places in the world, but not for northern Europe. Dry soils and vegetation led to reduced evaporation, increased heating of the surface, warming and drying of the air, contributing to less cloud cover and rain. Particularly, a threshold value of soil water content has been found for most locations, below which evaporation, heating, and daily maximum temperatures become significantly more sensitive to declining soil water. This is both a worrying indicator for the region in a warming climate and a potential source of additional predictability for the intensification of future heatwave events.

1. Introduction

The summer of 2018 saw a combination of drought and heat concentrated over northern Europe. The conditions had far-reaching economic and ecological impacts, with spring and summer dryness affecting crops and natural vegetation, leading to increased tree and forest mortality, and unprecedented wildfires in Sweden (Albergel et al., 2019; Rösner et al., 2019). The summer of 2018 was among the warmest, sunniest, and driest on record in the UK (Kendon et al., 2019). Figure 1 quantifies the drought and heatwave, showing the fraction of the 122 days spanning May through August 2018 that lie within the indicated tails of maximum 2 m air temperature anomalies and surface (top 7 cm) volumetric soil water content (VWC), based on the European Centre for Medium-range Weather Forecasts (ECMWF) fifth reanalysis (ERA5) from 1979 to 2018 (Hersbach et al., 2020). One would expect by chance a value of 0.05 at any location in the maximum temperature plot, and 0.25 for VWC. There is strong spatial correspondence between the two panels, but the core

Formal analysis: Paul A. Dirmeyer, Hollie M. Cooper
Investigation: Gianpaolo Balsamo, Eleanor M. Blyth, Ross Morrison
Methodology: Paul A. Dirmeyer
Resources: Gianpaolo Balsamo
Visualization: Hollie M. Cooper
Writing – original draft: Paul A. Dirmeyer
Writing – review & editing: Paul A. Dirmeyer, Gianpaolo Balsamo, Eleanor M. Blyth, Ross Morrison, Hollie M. Cooper
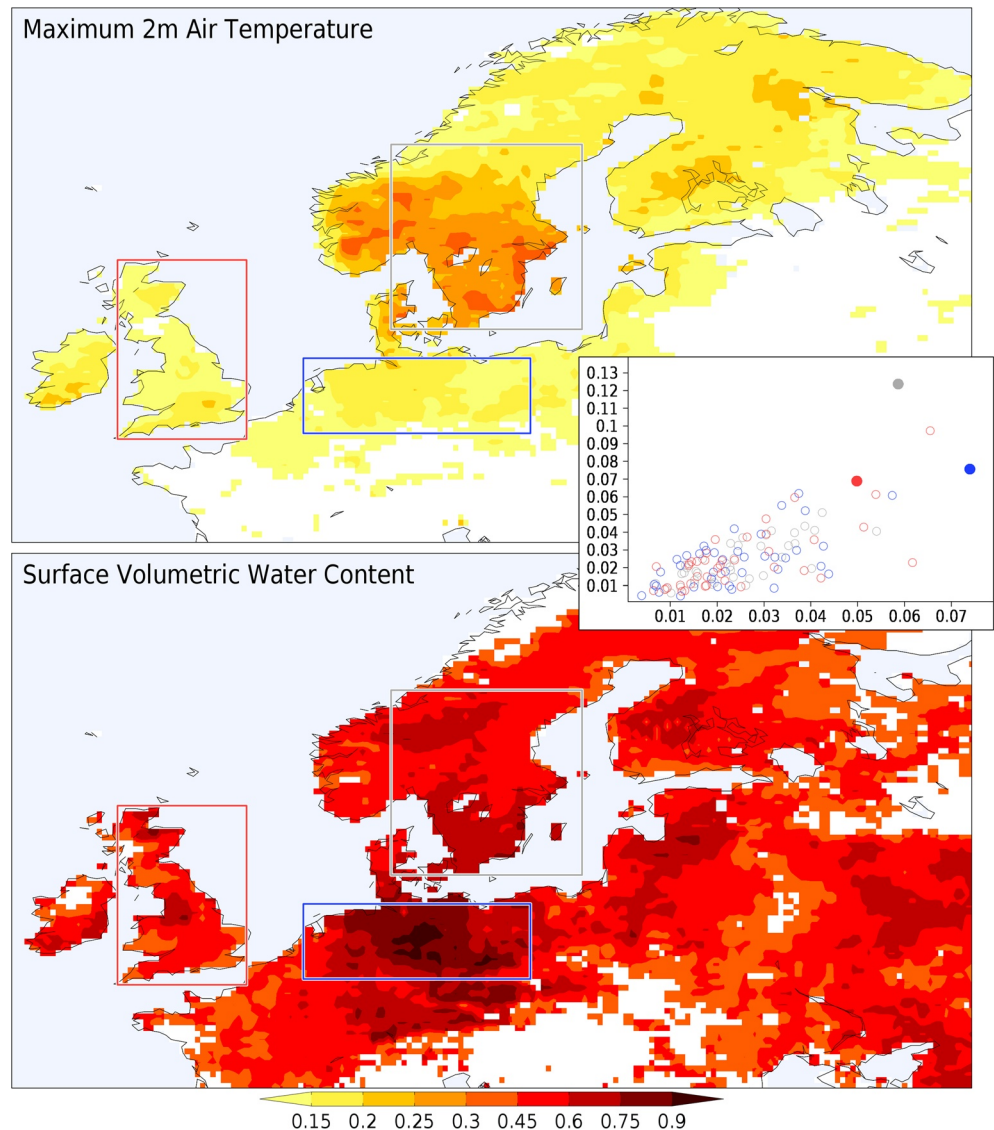
Figure 1. Fraction of days during May to August 2018 that are among 5% of warmest anomalies in maximum 2 m air temperature (top); among the 25% driest absolute surface layer VWC (bottom); compared to all days in May to August of 1979–2018 in ERA5. Colored areas are significant at the 99% confidence level; the VWC threshold is less strict for illustrative purposes and as it among several potential contributors to temperature extremes. Boxes outline regions defined for land-only area averages: Britain in red, Southern Scandinavia in gray, and Northern European Plain in blue. The inset shows the areal average of the fractions for VWC (*x*-axis) and temperature (*y*-axis) over land in the indicated rectangles for each of the 40 years; 2018 is indicated by filled circles.

of dry soils is clearly south of the core of high temperatures. In parts of Germany, nearly every day of May to August 2018 are in the driest quartile. For temperature, the most extreme conditions were over southern Scandinavia, where up to one third of the period was in the warmest 5% of anomalies of the previous 40 years. The inset shows how outstanding 2018 was (filled circles) over the three outlined regions, especially in terms of temperature. The one outlier among the points for 2018 is for Britain in 1995, which suffered an extreme heatwave and drought in the late summer (Parker et al., 1996).

The atmospheric circulation established conditions for anomalous heat and drought in the spring, with blocking high pressure and unfavorable moisture sources for precipitation beginning in April (Rösner et al., 2019). Synoptic features of the heatwave were well forecast up to 2 weeks in advance, and some aspects were evident out to 4 weeks (Magnusson et al., 2018), suggesting its origins lay in the large-scale

circulation (Kornhuber et al., 2019). The North Atlantic Oscillation (NAO) was in a positive phase, conducive to an anticyclonic circulation over northern Europe downstream from an amplified trough over Greenland (Hurrell et al., 2003). However, the extreme intensity and duration of the event suggest more was going on. An unusual amount of energy in high planetary wavenumbers may have amplified NAO impacts (Drouard et al., 2019). Studies suggest global warming was a significant contributor (Leach et al., 2020; Wehrli et al., 2020), but VWC anomalies over Britain could have had a role in the heatwave there (Petch et al., 2020).

There is generally a positive relationship between soil dryness and heat (Fischer et al., 2007; Hirsch et al., 2014; Hirschi et al., 2011; Philip et al., 2018; Santanello et al., 2011; Vautard et al., 2007). High air temperatures are conducive to drying soil by increasing evaporative demand. Dry soils heat more quickly than wet ones and may transmit absorbed radiant energy to the atmosphere as sensible heat more readily (Miralles et al., 2018). Dry soils also correspond to reduced evaporation, and if dry to a sufficient depth, reduced transpiration, further exacerbating the heat (Dirmeyer et al., 2015; Zscheischler et al., 2015). Such land-atmosphere (L-A) feedbacks alter the daytime atmospheric boundary layer, which ultimately affect cloud formation, precipitation, and the state of the free atmosphere above the boundary layer (Betts, 2004; Ek & Holtslag, 2004; Gentine et al., 2013; Santanello et al., 2007, 2011; Zhang et al., 2020). In this way, VWC can be a driver of extremes when water availability in the soil is a limiting factor for evapotranspiration (Santanello et al., 2018), an unusual situation in wet, cool, and cloudy northern Europe.

Recent years have seen several regional episodes of unprecedented heat over Europe (Russo et al., 2015). The combined hot and dry conditions experienced in northern Europe in 2018 are more typical of southern Europe, but such situations are projected to become more likely in a changing climate (Brabson et al., 2005; Lau & Nath, 2014; Leach et al., 2020; Samaniego et al., 2018; Seneviratne et al., 2006; Teuling, 2018; Zscheischler et al., 2018). Over northern Europe there is a particular concern, as precedent for such events is lacking. Although warning systems are being implemented, infrastructure is not well prepared to cope with heatwaves (Casanueva et al., 2019; Lass et al., 2011) and drought has historically been more impactful in southern Europe than northern Europe (Vicente-Serrano et al., 2014). While increasing trends in drought occurrence are indicated in both regions (Albergel et al., 2013), the unfamiliarity with such extremes in the North introduces additional challenges.

Modeling studies indicate that most of northern Europe remains in an energy-limited regime, even during the warmer summer months, not experiencing L-A feedbacks (Dirmeyer et al., 2009; Schwingshackl et al., 2018; Seneviratne et al., 2010). Thus, it is not usually a "hot spot" of L-A coupling like the Great Plains of North America or the Sahel region of Africa (Koster et al., 2006). Not only can such areas experience magnified responses to droughts and heat waves, the local climate may also react more strongly to land cover changes, agricultural practices, and climate change (Chen & Dirmeyer, 2020; Dirmeyer et al., 2013). Given the concurrent dry and warm conditions during the summer of 2018, we pose the question: Did northern Europe enter an unprecedented regime of L-A feedbacks—that is, did it become a coupling "hot spot" that may have intensified the heatwave? We combine analysis of in situ observational data and state of the art gridded reanalyzes to investigate the question. Section 2 describes the data used. Analysis techniques and metrics of L-A interaction are presented in Section 3. Results are shown in Section 4, followed by conclusions in Section 5.

2. Data

Hourly data from ERA5 for the 40-year period 1979–2018 are used in this study (Hersbach et al., 2020). The data are at a nominal 31 km resolution but have been interpolated to the full TL639 latitude-longitude grid (~0.28°) for this analysis. Vertical atmospheric resolution is also higher than any previous reanalysis, with 23 layers in the lowest 15% of the atmosphere by mass, and 55 layers in the lowest 70%.

ERA5 is the first reanalysis to assimilate satellite VWC data (de Rosnay et al., 2014). This assures better analyses of VWC, but also causes a lack of closure of the terrestrial water balance. Nevertheless, reanalyzes have been shown to perform well in regard to the simulation of L-A coupling metrics (Dirmeyer et al., 2018). ERA5 also provides the opportunity to examine the diurnal cycle with unprecedented detail as hourly data for all atmosphere and land surface variables are available. The diurnal cycle is a key element of coupled
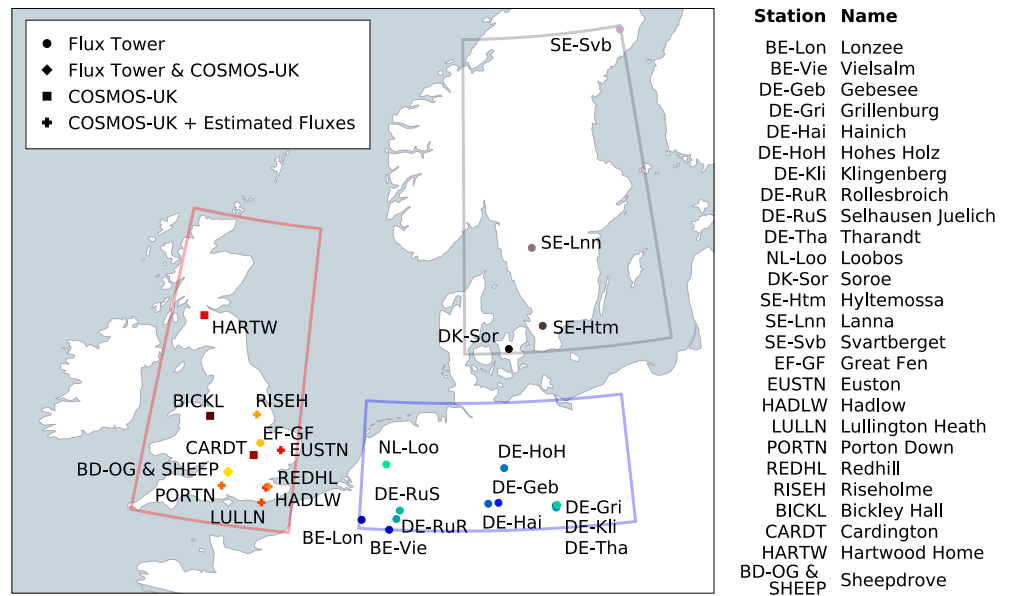
Figure 2. Locations of VWC and flux tower sites used in this study. Boxes outline the same regions defined in Figure 1.

L-A processes (Santanello et al., 2018). The 12-h data assimilation windows are shifted 6 h from the 0000 and 1200 UTC windows used in previous reanalyzes, and artifacts are sometimes evident toward the end of those windows, as is shown in Section 4. Note that because of lack of local budget closure in the reanalysis fields, exact balances cannot be calculated. Nevertheless, a good depiction of the temporal variability in budget terms is afforded.

For in situ analysis and comparisons over Europe, a combination of three data sets is used: (i) data from a network of eddy covariance flux towers operated in England by the UK Centre for Ecology and Hydrology (UKCEH Flux); (ii) data from a network of flux towers located across continental Europe (part of FLUX-NET); (iii) data from a network of meteorology and field-scale soil moisture monitoring stations distributed across the UK (COSMOS-UK). Figure 2 shows all observation sites that provided data for this analysis.

Additional flux tower data from a number of stations over continental Europe that were collected through 2018 and made consistent with the FLUXNET2015 archive format (Drought 2018 Team & ICOS Ecosystem Thematic Centre, 2020) have been obtained. Stations that include the full range of surface energy fluxes, air temperature and point-scale VWC in heatwave-stricken areas of northern Europe are used. Daily maximum temperatures are defined as the highest listed from 30-min data for each UTC-defined date.

Over Britain, data from two UKCEH grassland flux towers in southern England are used. The eddy covariance instrumentation combines Gill Instruments Ltd. Windmaster ultrasonic anemometer-thermometers and LI7500 series infrared gas analyzers (Li-COR Biosciences), alongside a standardized set of micrometeorological (radiation, air temperature, humidity, and pressure) and soil physics (temperature, point-scale VWC, and heat flux) sensors. Data processing and quality control follow standard methods of the global flux measurement community (Fratini & Mauder, 2014; Papale et al., 2006; Reichstein et al., 2005). Full details of the measurement sites, instrumentation, and data handling can be downloaded with the eddy covariance data sets (Morrison et al., 2019, 2020). The data duration is relatively short but provides ground truth to validate aspects of the coupled L-A behavior over Britain. As with ERA5, energy and water budgets from the eddy covariance sites do not close, but well-managed flux tower sites can still have great value for assessing local heatwave maintenance processes (Horst et al., 2019).

Data from UKCEH's COSMOS-UK network are also used. This network monitors field-scale VWC by utilizing a specialized cosmic-ray neutron sensor alongside collocated meteorological observations. The COSMOS-UK network has been developed since 2013 and provides subdaily field-scale VWC derived from counts of fast neutrons at the land surface (Stanley et al., 2019). Near-surface VWC is determined using

corrections for local atmospheric pressure, humidity, and background neutron intensity (Evans et al., 2016; Rosolem et al., 2013), and site-specific calibration is based on soil sampling and laboratory analysis (Evans et al., 2016). The COSMOS-UK network is more extensive than the UK flux towers, providing a distributed picture of near-surface water storage over Britain. Additionally, surface fluxes have been estimated for a subset of the COSMOS-UK network sites; where possible, sensible heat fluxes were derived from Windmaster ultrasonic anemometer-thermometers (Gill Instruments Ltd.). In contrast to the UKCEH Flux sites, no fast response hygrometers were deployed at COSMOS-UK sites. Latent heat flux was estimated as a residual from the other terms of the surface energy budget measured at these locations (e.g., LE = Rnet—G- H, Crowhurst et al., 2019). One COSMOS-UK location, Sheepdrove, has no flux estimates but is very near a UKCEH flux site.

Such an array of measurements provides ground truth at a number of locations around northern Europe to validate the behavior of ERA5 data, which provide complete coverage over the domain. The regions outlined in Figure 1 are chosen to enclose areas of large anomalies in temperature and soil moisture as well as a sizable number of observational stations. Tables S1 and S2 show the temporal correlations of daily time series between observations and ERA5 for field-scale VWC and daily maximum temperature at the COSMOS-UK sites, and for a number of variables at the sites with flux measurements. Correlations are calculated separately for 2017 and 2018 for the warm season period spanning 15 May through 15 October—a period of 154 days. ERA5 provides a trustworthy univariate representation of states and fluxes near the surface, as all correlations with COSMOS-UK sites are significant at the 99% confidence level, and more than 90% of the correlations at flux tower sites are significant at the 95% confidence level. Multivariate behavior, which is a crucial indicator of feedback processes linking land and atmosphere, is the topic of study here.

We focus on surface VWC rather than subsurface or column integrated VWC for several reasons. One, surface VWC is directly linked to sensible heat flux, which is a surface process that drives boundary layer growth and lower tropospheric warming (Betts, 2009). Two, COSMOS-UK instrumentation does not provide soil moisture profiles but a single value that is strongly weighted toward surface VWC. Lastly, although transpiration is a major component of latent heat flux, and its changes are strongly linked to root zone VWC, hysteresis and strongly varying time scales with depth have been found to yield less robust relationships with extreme heat (Benson & Dirmeyer, 2020).

3. Metrics

In order to investigate the possible role of L-A feedbacks on the 2018 heatwave and drought, we estimate several L-A coupling metrics as well as energy budget terms over affected areas. Daily anomalies in maximum temperature, surface VWC, and mean fluxes are calculated relative to a 40-year (1979–2018) climatological period for ERA5 data. For in situ data, comparisons between corresponding periods in 2018 and 2017 are made, as long records are not available from many of the stations. The period 15 May through 15 October is used for statistics and metrics calculations unless otherwise indicated.

Daily data are used to produce areal averages of key heat and moisture budget terms averaged over selected regions. Surface and atmospheric budgets are produced on an hourly timescale averaged over Britain to derive mean diurnal cycles of surface and vertical heating profiles. The ERA5 land mask is used to define the areal domains as land grid cells only, and averages across the grid cells are area weighted. For the vertical profiles of atmospheric variables, calculations are performed on the native ERA5 vertical levels, whose thicknesses at any location are proportional to surface pressure (i.e., a sigma coordinate in the vertical).

Lifted condensation level (LCL) is compared to the depth of the planetary boundary layer (PBL) to determine an LCL deficit (Santanello et al., 2011). We define it such that negative values indicate the PBL does not grow deep enough for condensation and cloud formation to occur. Such a shortfall can be caused by insufficient heating at the surface to generate the necessary buoyancy, low humidity of air near the surface, or a combination of both.

Transitions into moisture-limited regimes can greatly increase the process linkage between surface fluxes and air temperature (Benson & Dirmeyer, 2020; Denissen et al., 2020). Segmented regression is used to determine if there is a significant change in the bivariate relationship between VWC and extreme temperatures,
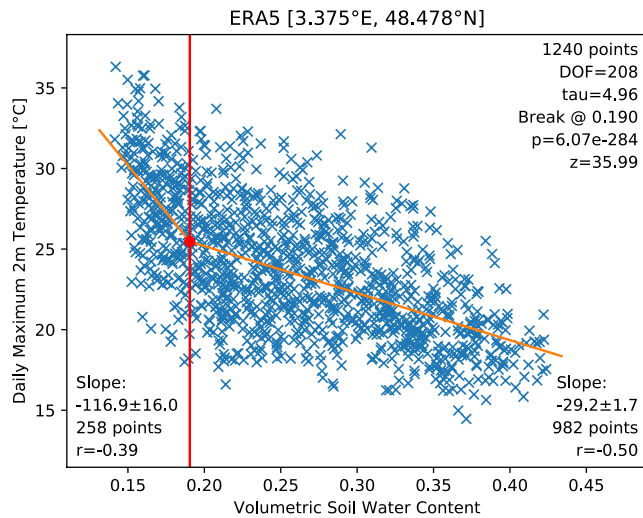
Figure 3. Relationship between daily maximum 2 m air temperature (dependent variable; ordinate) and surface VWC (abscissa) during July for 1979–2018 at a grid cell in France. Values in upper right refer to the total number of days (including VWC memory time scale "tau" in days and reduced degrees of freedom "DOF" due to VWC autocorrelation) and significance of the estimate of the threshold between two best fit linear regressions. Values in the lower corners show the estimated slopes ± standard error of estimates, number of points, and correlations for each segment—the fits for each segment are significant at the 99% confidence level.

which can be attributed to L-A feedbacks (Wu & Dirmeyer, 2020). Figure 3 provides an example at one ERA5 grid cell: for a specific time period (in this case a particular calendar month across 40 years), daily values of surface (0–7 cm) VWC and daily maximum air temperature are seen to have an inverse relationship, which is typical of many mid-latitude locations. To determine whether there is a difference in the slope of temperature estimated over different ranges of VWC, an optimization is calculated to minimize the RMS error of a pair of linear regressions over two segments which together cover the entire range of VWC at that location (V. M. Muggeo & Hajat, 2009; V. M. R. Muggeo, 2003). The criterion is that the two linear regressions must intersect at the same value of temperature (red dot) on the VWC threshold between the segments (red line). A least squares optimization to fit two line segments through the scatter of points in the phasespace as portrayed in Figure 3 is performed over four parameters: the slopes of the left (drier) and right (wetter) segments, the threshold values of VWC, and maximum temperature (Benson & Dirmeyer, 2020). Similar bivariate analyses are performed between VWC and surface fluxes.

Additional criteria are applied to filter the results. First, the two slopes must be significantly different. The variances of the estimates of the two slopes are averaged after adjusting down the sample size of N days by the VWC memory $_t$ in days (calculated as described in Dirmeyer et al., 2016) as $N/(\tau+1)$, to properly account for the degrees of freedom in the time series. From that, a z-score and p-score are calculated assuming a normal distribution of the potential errors in parameter estimates; p-scores of 0.01 or less are retained. Because we have in mind specific physical processes by which low VWC may affect surface fluxes and air temperature, we further constrain the slope of the linear regression to the left of the estimated threshold to be negative for temperature or sensible heat flux (SH), positive for latent heat flux (LH) or evaporative fraction (EF; the ratio of LH to the sum of LH and SH), and the slope must have a larger magnitude on the drier side of the threshold than the wetter side. We also check that there are at least 10 data points on either side of the threshold. Locations where the optimization fails to converge are omitted.

4. Results

The analysis is designed to determine whether locations in northern Europe moved into a regime where land surface feedbacks exacerbated drying and warming during 2018. For context, the evolution of monthly mean anomalies in surface VWC and maximum 2 m air temperature over northern Europe are shown in Figure S1 for the period of May to August 2018. Anomalously warm and dry conditions predominated over northern Europe in each month, but the patterns are not stationary. For VWC, only areas around northern Germany and the Baltic states are more than 0.03 m³/m³ drier than average in every month. Areas of positive temperature anomalies alternate between extreme heat over Scandinavia and lands adjacent to the North and Baltic seas (May, July) and less intense but still widespread warm anomalies anchored around Germany (June, August).

A more complete picture is given in Figures S2–S4, which portray anomalies in boundary layer states, surface energy, and moisture fluxes as represented in ERA5. Precipitation and VWC evolve similarly, reflecting persistent dry conditions, while anomalies in surface turbulent heat fluxes are much more prominent in SH than LH (Figure S2). Increases in SH correspond strongly with positive anomalies in downward shortwave radiation (Figure S3). Meanwhile, LH deficits are more closely linked to extremely dry soil, particularly during July and August. The planetary boundary tends to be slightly deeper in most locations (Figure S4) but is outpaced by the increases in the LCL, hampering cloud formation in areas where downward shortwave radiation increases.
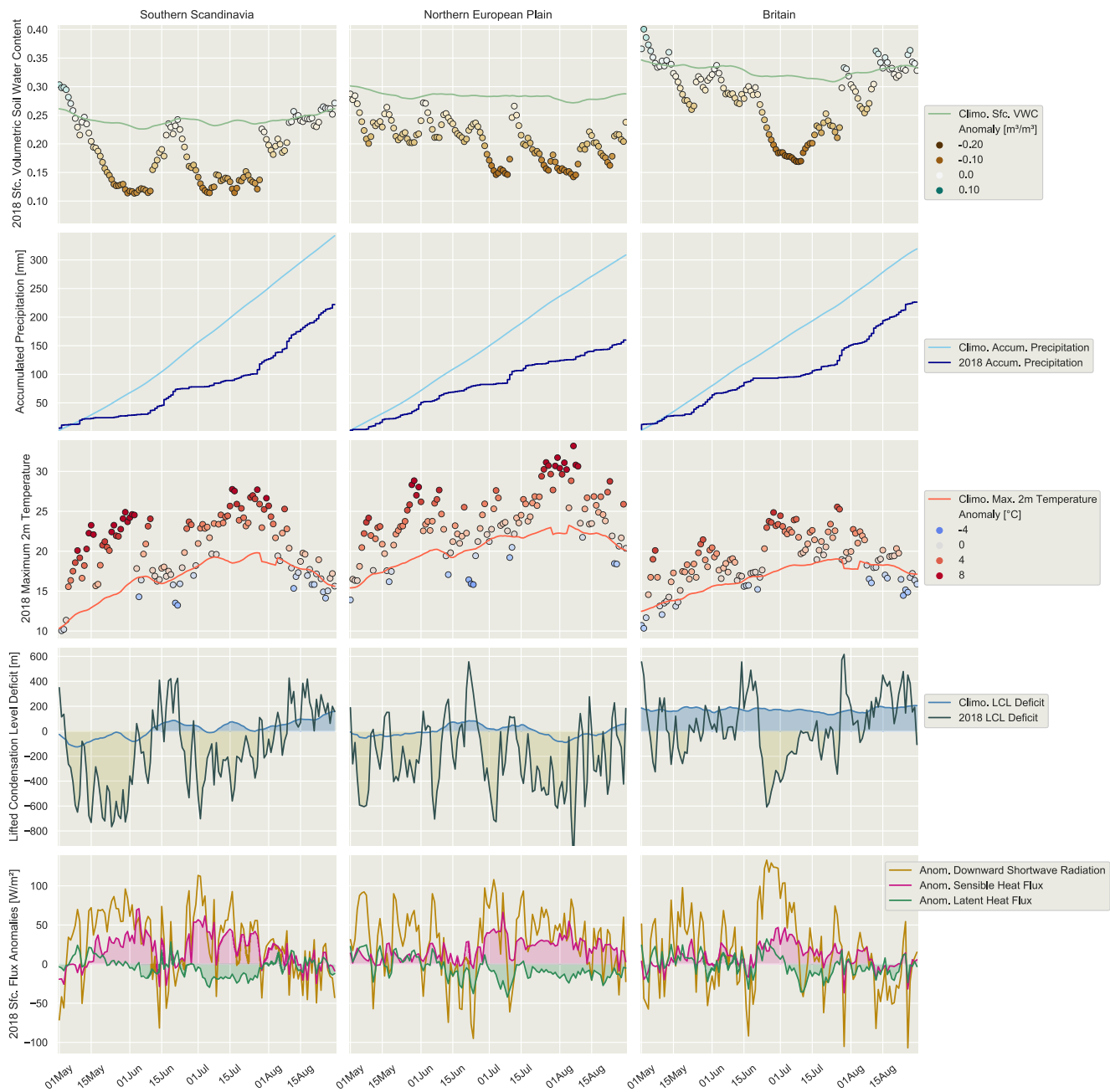
Figure 4. Area averages from ERA5 over land points in the indicated regions for daily surface layer VWC (top row), cumulative precipitation (second row), daily maximum 2 m air temperature (third row), LCL deficit (fourth row), and indicated surface energy balance terms (bottom row). In each panel, climatological values are indicated by a smooth (7-day centered running mean) line except in the bottom row where only anomalies are shown. In the first and third rows, color of dots indicates the magnitude of the anomaly.

There was considerable synoptic variability in heatwave and drought conditions during 2018. While the preceding figures give a good first-order impression of the magnitude and duration of warm dry conditions, the use of monthly means does not capture the nuances nor the peak periods. Area averages of daily time series during May to August in three areas that bore the brunt of the hot conditions: Southern Scandinavia (hereafter SSc), the Northern European Plain (NEP), and the island of Britain (outlined in Figures 1 and 2) are presented in Figure 4. The top row shows surface VWC for 2018 relative to its 40-year (1979–2018) climatological evolution, simply calculated as daily means with a centered 7-day running average applied. Each region was predominantly drier than normal, with the greatest anomalies during the first half of July.
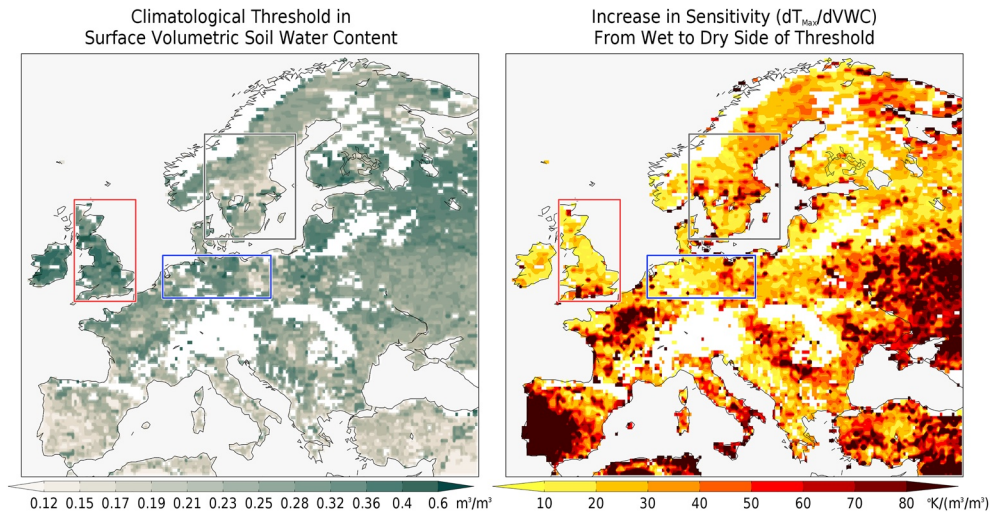
Figure 5. Left: Values of VWC estimated to be at the threshold regarding a significant change in the slope of the regression of daily maximum 2 m air temperature on VWC. Right: Change in the slope of the regression across the threshold. White areas fail to pass at least one of the criteria described in Section 3, with additional criteria that areas of organic (peat) soils are excluded and the estimated value of the maximum temperature at the threshold exceeds 10°C.

SSc also had a dry period during late May and early June that was as intense as during July, while NEP had very dry conditions in late July and August. Britain's driest period spanned late June to late July. The second row shows the climatological and 2018 accumulated precipitation from 1 May onwards, showing extreme shortfalls in all regions, although both SSc and Britain showed rainfall rates returning to normal in August (matching slopes of the curves).

Area averaged daily maximum temperatures are shown in the middle row of Figure 4. Positive anomalies dominate in all regions. Heatwave peaks correspond largely to the periods of low VWC. An exception occurred during late May over NEP, when temperatures were around 1°C–5°C above average, well below the 8°C–10°C range during the drier early July period. The fourth row shows the LCL deficit: negative values indicate the boundary layer does not grow deep enough for condensation and cloud formation to occur. The climatological lines show deficits hovering around 0 m over SSc and NEP, and consistent positive values over Britain suggesting clouds are likely to form above a growing boundary layer during every day of the period. During 2018, LCL deficits predominate over SSc and NEP, as well as during the most intense heatwave periods over Britain, when summer values were usually well below climatology. Figure S4 indicates the main cause was elevated LCL heights due to warm dry air, as PBL growth was not suppressed markedly during the period and was often above average.

The periods lacking convective clouds over land correspond to anomalous increases in downward shortwave radiation at the surface (Figure 4, bottom row). Those are also periods of enhanced SH flux in ERA5, but LH flux is not as responsive to the fluctuations in radiation. In fact, an interesting reversal occurs around July 1. Before that period, LH flux is clearly positively correlated with shortwave radiation, suggesting evaporation is limited by available energy. This is the typical situation across northern Europe, where L-A feedback is normally weak. After 1 July, LH flux becomes anticorrelated with both shortwave radiation and SH, indicative of a moisture-limited situation. This is a necessary condition for L-A feedback (Dirmeyer et al., 2015), suggesting the rare and possibly unprecedented situation that a L-A coupling "hot spot" over northern Europe may have exacerbated the heatwave.

To better establish the linkages between VWC and temperature extremes, we applied the segmented regression analysis described in Section 3 to the ERA5 VWC and maximum temperature data across northern Europe for the 1979–2018 period to produce a climatology of threshold statistics. Results were calculated separately for each month, but were found to be largely invariant (not shown); mean MJJA results are shown in Figure 5. The estimated threshold between two linear regressions is only shown where the criteria outlined in Section 3 are met. The segmented regression calculation fails to converge for 1%–2% of cells, and

only 2%–3% of cells fail to pass the significance test even with the degrees of freedom reduced in proportion to the VWC memory timescale. The most common criterion to be failed is that the slope is not steeper on the dry side of the threshold.

Thresholds in the higher range of local VWC (darker colors) correspond with smaller changes in slope (yellower colors in the right column). This situation is present over places like Ireland and southern Finland, indicating that extremely warm and dry conditions are too rare to allow detection of a stress threshold toward the dry end of the range. Much of northern and central Britain also falls in this regime. Soil texture is found to be a strong determinant of the VWC threshold value; the spatial correlation between model wilting point and the threshold over Europe is 0.50. Significant changes in slope (right panel of Figure 5) are indicative of a hypersensitive realm at very low VWC where daytime temperatures can elevate markedly as soil dries.

To verify the bivariate relationships related to L-A coupling shown so far using ERA5 data, we examine in situ data during 2018 and the more normal summer of 2017. If we find that the observed relationships between links in the process chain of L-A coupling (Santanello et al., 2018) are represented well in ERA5 over those locations, we may use the reanalyzes with greater confidence to extrapolate conclusions to the rest of northern Europe. Figure 6 summarizes these comparisons.

The expectation is that low VWC feeding back on extreme daily maximum temperatures T_{Max} will result in a steeper slope dT_{Max}/dVWC than when VWC is high (above the threshold). This is found at 19 of the 23 stations and for 20 of the 23 ERA5 grid cells (points to the left of the dotted $x = y$ line in the top panels of Figure 6). The locations where the expectation is not fulfilled are not the same in the two data sets. The differences in sensitivity between wet and dry soil conditions is typically greater in the station observations than ERA5 grid cells, which may reflect the area-averaged nature of the reanalysis data (each grid cell has an area of nearly 10^3 km^2). The fit of regressions over dry soils is also typically stronger (Figure 6, middle panels) suggesting high confidence in the dry soil driven heat sensitivity. Much of the data informing the dry-side relationship between VWC and extreme temperature comes from 2018; the lower panels of Figure 6 show that there were near universally more dry days during May to August than in 2017, enhancing L-A coupling.

The linkage from VWC to daytime maximum temperature operates through changing surface fluxes of heat and moisture. Figure S5 shows the segmented regression relationships between EF and VWC at the station sites is comparable to that found when maximum temperature and VWC are considered. The strong resemblance between threshold VWC shown in Figures S6 and 5 (spatial correlation across unmasked cells is 0.83) shows that this is not confined to the limited number of stations. Changes in sensitivity share the broad north-south gradient. The values of the thresholds are very similar regardless of whether maximum surface temperature, EF or SH are regressed on volumetric VWC (Table S3). Differences are quite small between thresholds estimated with any variable except LH flux, which shows a strong positive bias (threshold occurring at a higher value of VWC, likely due to the effect of subsurface soil moisture on transpiration) and root mean square errors 15%–45% higher than other flux variables. The relationship between VWC and SH appears to be the main factor for temperature sensitivity amplification during combined drought heatwave cases, supporting in a temporal sense the result suggested spatially in Figures 5 and S6.

The ERA5 estimates consistently show a weaker sensitivity than observations on the dry side of the threshold and less of a change in sensitivity between the wet and dry sides of the threshold. Overall, it appears that ERA5 underestimates the impact of very dry soils on extreme temperatures, particularly over Britain. A reason for the weaker coupling to drought-T_{Max} in ERA5 might be the lack of VWC-vegetation feedback, since ERA5 adopts a monthly climatology of leaf area index (Boussetta et al., 2013). Moreover, recent findings by Nogueira et al. (2020) highlight the interplay of vegetation cover and state in further enhancing surface temperatures. Although not shown here, the VWC threshold values found at individual sites in both observations and ERA5 for 2018 are more stable and in better agreement with the 2-year estimate than are the 2017-based values, which include few dry days in the sample that can exhibit L-A feedback.

The fraction of days during May through August 2018 that lie on the dry side of the climatologically estimated thresholds based on both maximum temperature and EF are shown in Figure 7. In each case, the climatological fraction of days is subtracted, so that positive values suggest more days than average in the hypersensitive VWC regime, and thus enhanced L-A feedbacks, during 2018. Comparison to Figure 1 shows how this metric synthesizes the extremes in VWC and temperature, as well as providing a spatial depiction of regions where
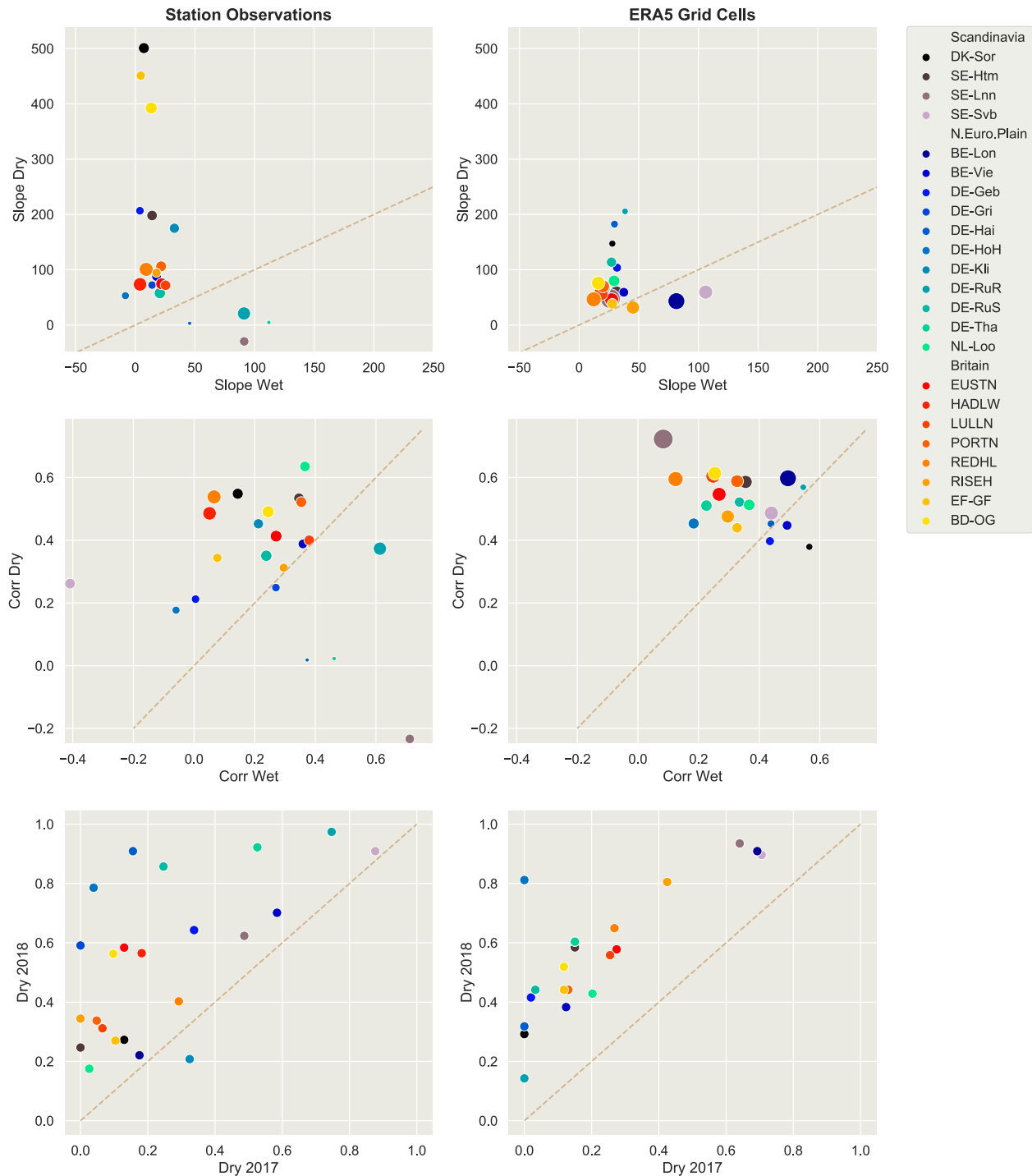
Figure 6. Relationships for in situ stations (left column) and their corresponding ERA5 grid cells (right column) between the sensitivity (slope; $K/[m^3m^{-3}]$) dT_{Max}/dSM on the wet and dry sides of the thresholds (top); correlation of the points in the linear regression of T_{Max} on SM on each side of the threshold (middle); Fraction of days during MJJA on the dry side of the threshold during the period 15 May through 15 October in 2018 versus 2017 (bottom). In the first two rows, slopes and correlations are multiplied by -1 for clarity, and the size of the symbol is proportional to the confidence in the dry-side slope defined as the slope divided by the standard error in the estimation of the slope.

L-A feedbacks could have exacerbated the hot conditions in 2018. Large portions of northern Europe experienced at least a 25% increase in the number of critically dry soil days, including not only the three regions highlighted earlier in the study, but also over large areas of the eastern Baltic and western Eurasian steppes. Very few areas had a decrease in the number of critically dry days during the warm season of 2018.
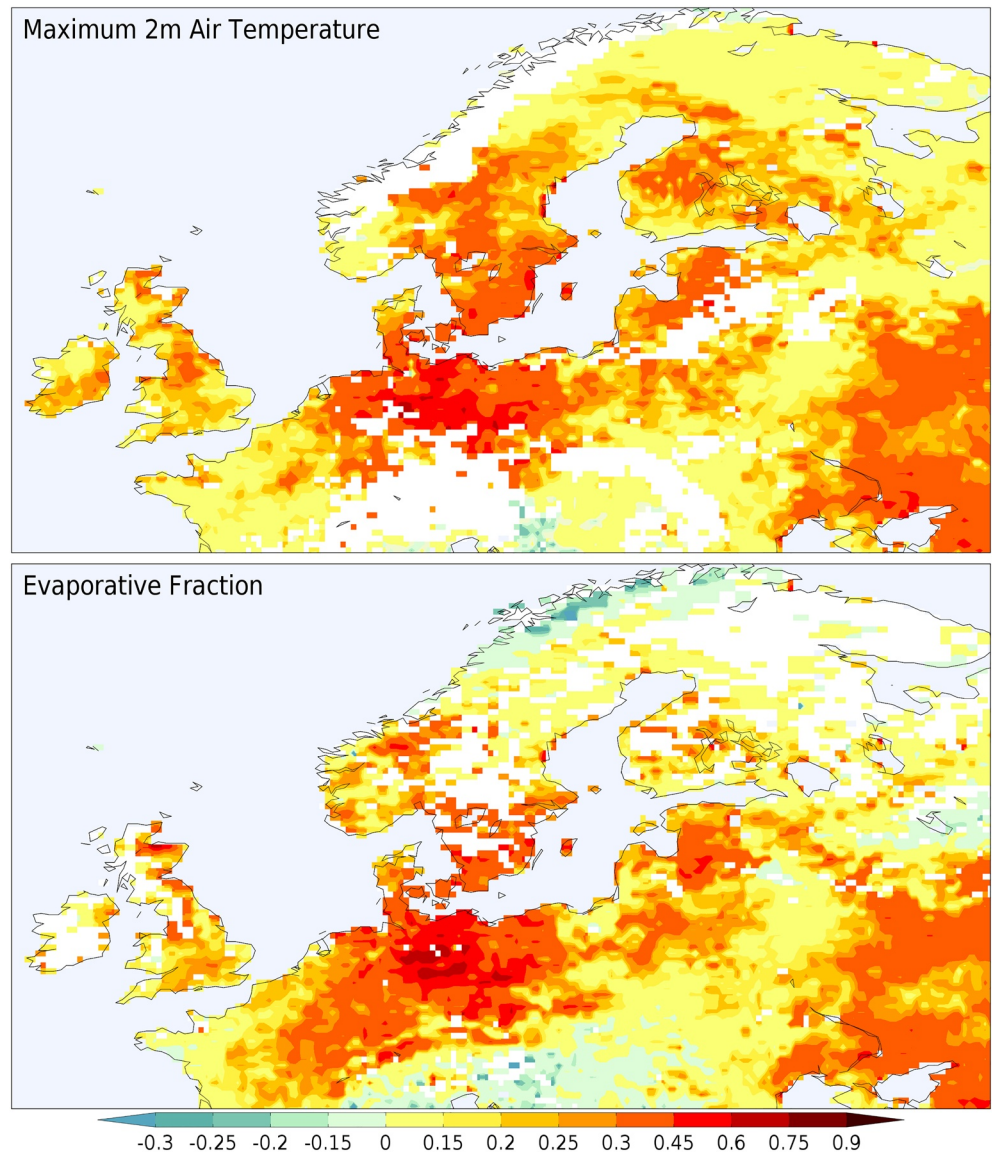
Figure 7. Increase in the fraction of days during May to August 2018 on the dry side of the surface VWC threshold based on ERA5 daily maximum temperature (top) and evaporative fraction (bottom) compared to the 1979–2018 average. Masked areas fail to meet the screening criteria described in Section 3 in all 4 months.

The representativeness of ERA5 at field sites within each of the regions is summarized in Table S4. Generally, the ranked correlations across stations in each region are very high. The one situation where they are not across NEP for the T_{Max} sensitivity to VWC on the dry side of the threshold. Also shown is a comparison of the interstation variability of the threshold VWC values compared to how the threshold estimates differ depending on which variable is regressed against VWC. Differences between stations are generally larger than differences among approaches to estimating thresholds at each station, suggesting high confidence in both the threshold methodology and the fidelity of ERA5 to represent the processes linking VWC variations to heatwave intensity.

Finally, to understand how the surface or terrestrial leg of the process chain of L-A coupling (Dirmeyer, 2011) may connect to the atmospheric leg to reinforce the large-scale dynamical drivers for the heatwave, we focus on the vertical structure of the atmosphere in ERA5 data over Britain. Figure 8 provides a diurnal Hovmöller diagram of the vertical profile of diabatic heating from ERA5, averaged over the land grid cells of the Britain box. The mean warm-season diurnal profile for the 39 years prior to 2018 shows a warming
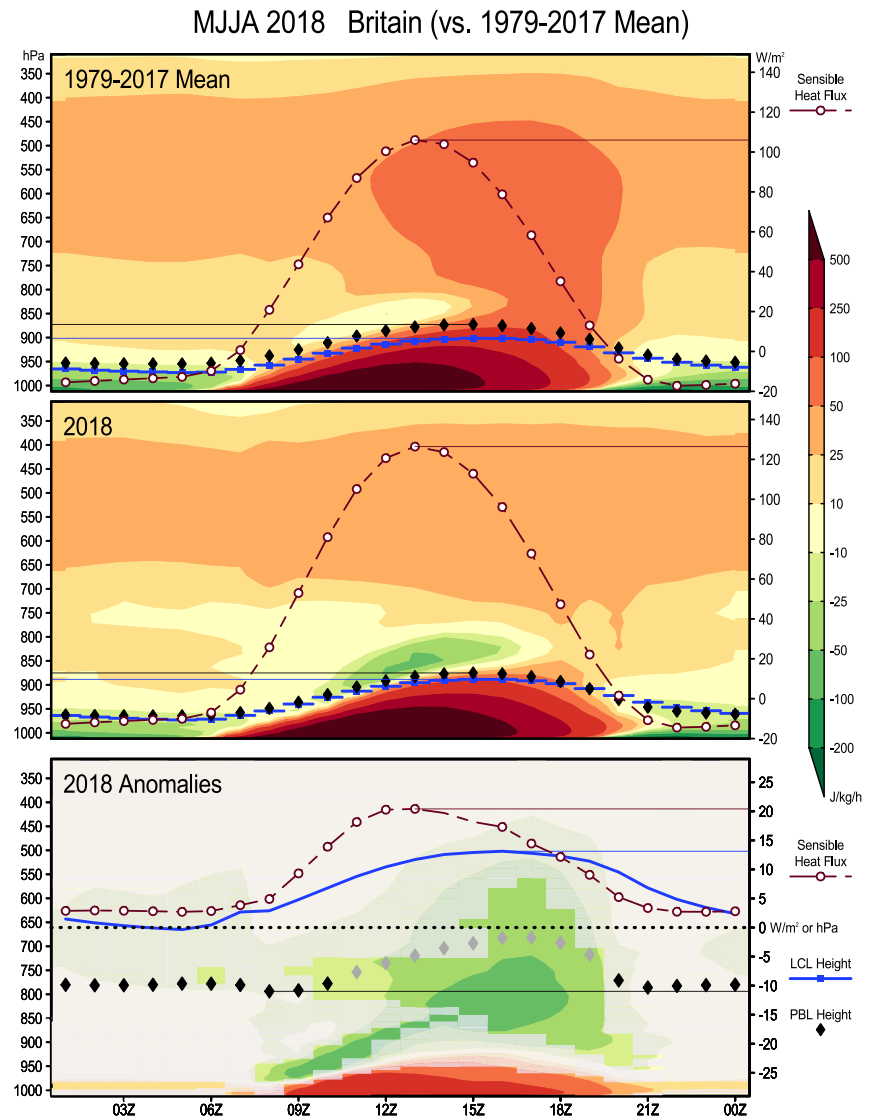
Figure 8. Time-height (model pseudo-pressure coordinate, scale on the left; see Section 2 for details) diagram of hourly heat budget terms averaged over land grid cells of Britain (red box in Figure 1) from ERA5 data. Shading is total diabatic heating per hour—insignificant anomalies for 2018 are grayed out in the bottom panel. Lines and/or symbols show surface sensible heat flux, LCL height, and PBL height as indicated, and thin horizontal lines mark daily extremes tailing to the appropriate scale. In the bottom panel, faint or missing hourly markers indicate lack of significance of the anomaly. All significances are at 95% confidence levels.

and deepening of the boundary layer from sunrise through the afternoon, with shallow cooling at night. Climatologically, there is convective warming that breaks through the boundary layer in the late afternoon, leading to enhanced mid-tropospheric warming due to latent heat release. In fact, there is weak warming in the mid-troposphere at all times of day due to condensation in clouds. Climatologically, the boundary layer height is above the LCL; another indication that Britain is more often cloudy than not. Peak SH flux occurs an hour after noon.

In 2018, daytime boundary layer heating is anomalously strong during the day and cooling is weaker at night. There is less heating of the troposphere above the boundary layer due to less latent heat release in clouds and more radiative cooling balancing subsidence in the persistent ridge (Yiou et al., 2020). There is actually net cooling above the boundary layer from mid-morning to mid-afternoon due to entrainment of lower potential temperature air from below. The LCL is higher while the boundary layer depth is lower, and

surface SH flux is about 20% greater. Figure S7 presents a similar analysis for moisture fluxes—the anomalies centered around 08 and 20 UTC are artifacts of the data assimilation cycle. Otherwise, more aggressive heating of the boundary layer from the land surface over Britain appears to lead to stronger moisture diffusion and entrainment into the free atmosphere without condensation, but stronger nighttime drying of the lower troposphere and little change in LH flux.

5. Conclusions

In this study, we have used a combination of high-quality reanalyzes and in situ measurements of VWC, temperature, and surface fluxes to demonstrate the existence of a threshold in the range of VWC below which the sensitivity of the atmosphere to drying soils substantially increases, providing a potentially strong positive feedback mechanism by which the land surface may exacerbate heatwaves during drought conditions. Such a threshold is crossed nearly every year in many locations, for example across southern Europe. We diagnose the presence of this transition during the 2018 drought and heatwave over northern Europe, an area that normally does not enter into conditions amenable to such positive L-A feedbacks (Santanello et al., 2018; Seneviratne et al., 2010).

During 2018, exceptionally dry conditions spread throughout much of northern Europe in concurrence with multiple prolonged episodes of extreme heat. Segmented regression analysis uninformed by physical processes identifies stable values of thresholds in the range of surface VWC at most locations, including VWC monitoring sites in Britain and flux stations across northern Europe. The values of surface VWC signifying the threshold in heatwave sensitivity are largely invariant from month to month and are also very similar whether the regressions are trained with dependent variable being daily maximum air temperature, SH or EF. There are greater variations when LH is the dependent variable, suggesting the loss of evaporative cooling is less of a regulator of extreme heat than the direct warming of desiccated land surfaces and transfer of that heat to the atmosphere.

Patterns over Europe in ERA5 show L-A feedbacks probably exacerbated the extreme heat during 2018. However, field data suggest ERA5 may actually underestimate the increase of sensitivity of extreme temperatures to declining VWC in very dry conditions, so the European maps based on ERA5 data may not represent the full potential impact of drying soils on heatwaves. The present study cannot establish the degree to which scale differences between the flux tower and COSMOS-UK VWC sites (with a footprint no larger than 1 km^2) and ERA5 grid cells (around 10^3 km^2) contribute to the discrepancies. Few areas of Europe were free from dry conditions during the summer of 2018, so a combination of local land-driven feedback mechanisms suggested here and nonlocal mechanisms (Berg et al., 2016; Miralles et al., 2018; Schumacher et al., 2019) likely contributed to the observed extremes. If connected to climate change, heat waves exacerbated by L-A feedbacks may become a new and common occurrence across northern Europe.

The hypersensitivity of extreme temperatures to declining VWC below a determinable threshold can provide a source of predictability for severe heatwaves. It should be realized that the impact of dry soil is to shift the probability distribution of extreme temperatures; it is one of several factors that can contribute to heatwaves. Soil processes need to be represented correctly and accurately in forecast models to replicate the timing of increased sensitivity, and proper initialization of those forecast models with real-time VWC conditions can contribute to increased forecast skill and improved early warning of heatwaves, even in regions which have historically been safe from such extremes.

Data Availability Statement

References

Albergel, C., Dorigo, W., Reichle, R. H., Balsamo, G., de Rosnay, P., Muñoz-Sabater, J., et al. (2013). Skill and global trend analysis of soil moisture from reanalyses and microwave remote sensing. *Journal of Hydrometeorology*, *14*(4), 1259–1277. https://doi.org/10.1175/JHM-D-12-0161.1

Albergel, C., Dutra, E., Bonan, B., Zheng, Y., Munier, S., Balsamo, G., et al. (2019). Monitoring and forecasting the impact of the 2018 summer heatwave on vegetation. *Remote Sensing*, *11*(5), 520. https://doi.org/10.3390/rs11050520

Benson, D. O., & Dirmeyer, P. A. (2020). Characterizing the relationship between temperature and soil moisture extremes and their role in the exacerbation of heatwaves over the contiguous United States. *Journal of Climate*, *34*, 1–39. https://doi.org/10.1175/JCLI-D-20-0440.1

Berg, A., Findell, K., Lintner, B., Giannini, A., Seneviratne, S. I., Hurk, B. van den, et al. (2016). Land–atmosphere feedbacks amplify aridity increase over land under global warming. *Nature Climate Change*, *6*(9), 869–874. https://doi.org/10.1038/nclimate3029

Betts, A. K. (2004). Understanding hydrometeorology using global models. *Bulletin of the American Meteorological Society*, *85*(11), 1673–1688. https://doi.org/10.1175/BAMS-85-11-1673

Betts, A. K. (2009). Land-surface-atmosphere coupling in observations and models. *Journal of Advances in Modeling Earth Systems*, *1*, 4. https://doi.org/10.3894/JAMES.2009.1.4

Boussetta, S., Balsamo, G., Beljaars, A., Kral, T., & Jarlan, L. (2013). Impact of a satellite-derived leaf area index monthly climatology in a global numerical weather prediction model. *International Journal of Remote Sensing*, *34*(9–10), 3520–3542. https://doi.org/10.1080/01431161.2012.716543

Brabson, B. B., Lister, D. H., Jones, P. D., & Palutikof, J. P. (2005). Soil moisture and predicted spells of extreme temperatures in Britain. *Journal of Geophysical Research*, *110*(D5), D05104. https://doi.org/10.1029/2004JD005156

Casanueva, A., Burgstall, A., Kotlarski, S., Messeri, A., Morabito, M., Flouris, A. D., et al. (2019). Overview of existing heat-health warning systems in Europe. *International Journal of Environmental Research and Public Health*, *16*(15), 2657. https://doi.org/10.3390/ijerph16152657

Chen, L., & Dirmeyer, P. A. (2020). Distinct impacts of land use and land management on summer temperatures. *Frontiers in Earth Science*, *8*, 245. https://doi.org/10.3389/feart.2020.00245

Crowhurst, D., Morrison, R., Evans, J., Cooper, H., Cumming, A., Fry, M., & Boorman, D. (2019). Actual evaporation data system for COSMOS-UK. Workshop presented at the Hydro-JULES: Next generation land surface and hydrological predictions. The Royal Society, London. Retrieved from http://nora.nerc.ac.uk/id/eprint/525105/

Denissen, J. M. C., Teuling, A. J., Reichstein, M., & Orth, R. (2020). Critical soil moisture derived from satellite observations over Europe. *Journal of Geophysical Research: Atmospheres*, *125*(6), e2019JD031672. https://doi.org/10.1029/2019JD031672

de Rosnay, P., Balsamo, G., Albergel, C., Muñoz-Sabater, J., & Isaksen, L. (2014). Initialisation of land surface variables for numerical weather prediction. *Surveys in Geophysics*, *35*(3), 607–621. https://doi.org/10.1007/s10712-012-9207-x

Dirmeyer, P. A. (2011). The terrestrial segment of soil moisture-climate coupling. *Geophysical Research Letters*, *38*(16), L16702. https://doi.org/10.1029/2011GL048268

Dirmeyer, P. A., Balsamo, G., & Peters-Lidard, C. D. (2015). Land-atmosphere interactions and the water cycle. In G. Brunet, S. Jones, & P. M. Ruti (Eds.), *Seamless prediction of the Earth system: From minutes to months* (pp. 145–154). Geneva, Switzerland: World Meteorological Organization.

Dirmeyer, P. A., Chen, L., Wu, J., Shin, C.-S., Huang, B., Cash, B. A., et al. (2018). Verification of land–atmosphere coupling in forecast models, reanalyses, and land surface models using flux site observations. *Journal of Hydrometeorology*, *19*(2), 375–392. https://doi.org/10.1175/JHM-D-17-0152.1

Dirmeyer, P. A., Jin, Y., Singh, B., & Yan, X. (2013). Evolving land–atmosphere interactions over North America from CMIP5 simulations. *Journal of Climate*, *26*(19), 7313–7327. https://doi.org/10.1175/JCLI-D-12-00454.1

Dirmeyer, P. A., Schlosser, C. A., & Brubaker, K. L. (2009). Precipitation, recycling, and land memory: An integrated analysis. *Journal of Hydrometeorology*, *10*(1), 278–288. https://doi.org/10.1175/2008JHM1016.1

Dirmeyer, P. A., Wu, J., Norton, H. E., Dorigo, W. A., Quiring, S. M., Ford, T. W., et al. (2016). Confronting weather and climate models with observational data from soil moisture networks over the United States. *Journal of Hydrometeorology*, *17*(4), 1049–1067. https://doi.org/10.1175/JHM-D-15-0196.1

Drouard, M., Kornhuber, K., & Woollings, T. (2019). Disentangling dynamic contributions to Summer 2018 anomalous weather over Europe. *Geophysical Research Letters*, *46*(21), 12537–12546. https://doi.org/10.1029/2019GL084601

Drought 2018 Team, & ICOS Ecosystem Thematic Centre. (2020). *Drought-2018 ecosystem eddy covariance flux product for 52 stations in FLUXNET-Archive format (Version 2.0) [Collection of FLUXNET product ZIP archives]*. https://doi.org/10.18160/YVR0-4898

Ek, M. B., & Holtslag, A. A. M. (2004). Influence of soil moisture on boundary layer cloud development. *Journal of Hydrometeorology*, *5*(1), 86–99. https://doi.org/10.1175/1525-7541(2004)005<0086:IOSMOB>2.0.CO;2

Evans, J. G., Ward, H. C., Blake, J. R., Hewitt, E. J., Morrison, R., Fry, M., et al. (2016). Soil water content in southern England derived from a cosmic-ray soil moisture observing system – COSMOS-UK. *Hydrological Processes*, *30*(26), 4987–4999. https://doi.org/10.1002/hyp.10929

Fischer, E. M., Seneviratne, S. I., Lüthi, D., & Schär, C. (2007). Contribution of land-atmosphere coupling to recent European summer heat waves. *Geophysical Research Letters*, *34*(6), L06707. https://doi.org/10.1029/2006GL029068

Fratini, G., & Mauder, M. (2014). Towards a consistent eddy-covariance processing: An intercomparison of EddyPro and TK3. *Atmospheric Measurement Techniques*, *7*(7), 2273–2281. https://doi.org/10.5194/amt-7-2273-2014

Gentine, P., Holtslag, A. A. M., D'Andrea, F., & Ek, M. (2013). Surface and atmospheric controls on the onset of moist convection over land. *Journal of Hydrometeorology*, *14*(5), 1443–1462. https://doi.org/10.1175/JHM-D-12-0137.1

Hersbach, H., Bell, B., Berrisford, P., Hirahara, S., Horányi, A., Muñoz-Sabater, J., et al. (2020). The ERA5 global reanalysis. *Quarterly Journal of the Royal Meteorological Society*, *146*(730), 1999–2049. https://doi.org/10.1002/qj.3803

Hirsch, A. L., Pitman, A. J., Seneviratne, S. I., Evans, J. P., & Haverd, V. (2014). Summertime maximum and minimum temperature coupling asymmetry over Australia determined using WRF. *Geophysical Research Letters*, *41*(5), 1546–1552. https://doi.org/10.1002/2013GL059055

Hirschi, M., Seneviratne, S. I., Alexandrov, V., Boberg, F., Boroneant, C., Christensen, O. B., et al. (2011). Observational evidence for soil-moisture impact on hot extremes in southeastern Europe. *Nature Geoscience*, *4*(1), 17–21. https://doi.org/10.1038/ngeo1032

Horst, S. V. J. van der, Pitman, A. J., Kauwe, M. G. D., Ukkola, A., Abramowitz, G., & Isaac, P. (2019). How representative are FLUXNET measurements of surface fluxes during temperature extremes? *Biogeosciences*, *16*(8), 1829–1844. https://doi.org/10.5194/bg-16-1829-2019

Hurrell, J. W., Kushnir, Y., Ottersen, G., & Visbeck, M. (2003). An overview of the North Atlantic oscillation. In James W. Hurrell, Y. Kushnir, G. Ottersen & M. Visbeck (Eds.), *The North Atlantic Oscillation: Climatic significance and environmental impact* (Vol. *134*, pp. 1–35). American Geophysical Union (AGU). https://doi.org/10.1029/134GM01

Kendon, M., McCarthy, M., Jevrejeva, S., Matthews, A., & Legg, T. (2019). State of the UK climate 2018. *International Journal of Climatology*, *39*(S1), 1–55. https://doi.org/10.1002/joc.6213

Kornhuber, K., Osprey, S., Coumou, D., Petri, S., Petoukhov, V., Rahmstorf, S., & Gray, L. (2019). Extreme weather events in early summer 2018 connected by a recurrent hemispheric wave-7 pattern. *Environmental Research Letters*, *14*(5), 054002. https://doi.org/10.1088/1748-9326/ab13bf

Koster, R. D., Sud, Y. C., Guo, Z., Dirmeyer, P. A., Bonan, G., Oleson, K. W., et al. (2006). GLACE: The global land–atmosphere coupling experiment. Part I: overview. *Journal of Hydrometeorology*, *7*(4), 590–610. https://doi.org/10.1175/JHM510.1

Lass, W., Haas, A., Hinkel, J., & Jaeger, C. (2011). Avoiding the avoidable: Towards a European heat waves risk governance. *International Journal of Disaster Risk Science*, *2*(1), 1–14. https://doi.org/10.1007/s13753-011-0001-z

Lau, N.-C., & Nath, M. J. (2014). Model simulation and projection of European heat waves in present-day and future climates. *Journal of Climate*, *27*(10), 3713–3730. https://doi.org/10.1175/JCLI-D-13-00284.1

Leach, N. J., Li, S., Sparrow, S., van Oldenborgh, G. J., Lott, F. C., Weisheimer, A., & Allen, M. R. (2020). Anthropogenic influence on the 2018 Summer warm spell in Europe: The impact of different spatio-temporal scales. *Bulletin of the American Meteorological Society*, *101*(1), S41–S46. https://doi.org/10.1175/BAMS-D-19-0201.1

Magnusson, L., Ferranti, L., & Vamborg, F. (2018). Forecasting the 2018 European heatwave. *ECMWF Newsletter*, *157*, 2–3.

Miralles, D. G., Gentine, P., Seneviratne, S. I., & Teuling, A. J. (2018). Land–atmospheric feedbacks during droughts and heatwaves: State of the science and current challenges. *Annals of the New York Academy of Sciences*, *1436*(1), 19–35. https://doi.org/10.1111/nyas.13912

Morrison, R., Cooper, H., Cumming, A., Evans, C., Thomton, J., Winterbourn, B., et al. (2020). *Eddy covariance measurements of carbon dioxide, energy and water fluxes at a cropland and a grassland on lowland peat soils*. UK: East Anglia. Retrieved from https://catalogue.ceh.ac.uk/id/2fe84b80-117a-4b19-a1f5-71bbd1dba9c9

Morrison, R., Cooper, H., Cumming, A., Scarlett, P., Thornton, J., & Winterbourn, B. (2019). *Eddy covariance measurements of carbon dioxide, energy and water fluxes at an organically managed grassland*. Berkshire, UK: Retrieved from https://catalogue.ceh.ac.uk/id/5a93161f-0124-4650-a2c9-7e8aaea7e6bb

Muggeo, V. M., & Hajat, S. (2009). Modelling the non-linear multiple-lag effects of ambient temperature on mortality in Santiago and Palermo: A constrained segmented distributed lag approach. *Occupational and Environmental Medicine*, *66*(9), 584–591. https://doi.org/10.1136/oem.2007.038653

Muggeo, V. M. R. (2003). Estimating regression models with unknown break-points. *Statistics in Medicine*, *22*(19), 3055–3071. https://doi.org/10.1002/sim.1545

Nogueira, M., Albergel, C., Boussetta, S., Johannsen, F., Trigo, I. F., Ermida, S. L., et al. (2020). Role of vegetation in representing land surface temperature in the CHTESSEL (CY45R1) and SURFEX-ISBA (v8.1) land surface models: A case study over Iberia. *Geoscientific Model Development Discussions*, *13*(9), 3975–3993. https://doi.org/10.5194/gmd-2020-49

Papale, D., Reichstein, M., Aubinet, M., Canfora, E., Bernhofer, C., Kutsch, W., et al. (2006). Towards a standardized processing of Net Ecosystem Exchange measured with eddy covariance technique: Algorithms and uncertainty estimation. *Biogeosciences*, *3*(4), 571–583. https://doi.org/10.5194/bg-3-571-2006

Parker, D. E., Horton, E. B., Cullum, D. P. N., & Folland, C. K. (1996). Global and regional climate in 1995. *Weather*, *51*(6), 202–210. https://doi.org/10.1002/j.1477-8696.1996.tb06214.x

Petch, J. C., Short, C. J., Best, M. J., McCarthy, M., Lewis, H. W., Vosper, S. B., & Weeks, M. (2020). Sensitivity of the 2018 UK summer heatwave to local sea temperatures and soil moisture. *Atmospheric Science Letters*, *21*(3), e948. https://doi.org/10.1002/asl.948

Philip, S. Y., Kew, S. F., Hauser, M., Guillod, B. P., Teuling, A. J., Whan, K., et al. (2018). Western US high June 2015 temperatures and their relation to global warming and soil moisture. *Climate Dynamics*, *50*(7–8), 2587–2601. https://doi.org/10.1007/s00382-017-3759-x

Reichstein, M., Falge, E., Baldocchi, D., Papale, D., Aubinet, M., Berbigier, P., et al. (2005). On the separation of net ecosystem exchange into assimilation and ecosystem respiration: Review and improved algorithm. *Global Change Biology*, *11*(9), 1424–1439. https://doi.org/10.1111/j.1365-2486.2005.001002.x

Rösner, B., Benedict, I., van Heerwaarden, C., Weerts, A., Hazeleger, W., Bissolli, P., & Trachte, K. (2019). The long heat wave and drought in Europe in 2018. *Bulletin of the American Meteorological Society*, *100*(9), S222–S223. https://doi.org/10.1175/2019BAMSStateoftheClimate.1

Rosolem, R., Shuttleworth, W. J., Zreda, M., Franz, T. E., Zeng, X., & Kurc, S. A. (2013). The effect of atmospheric water vapor on neutron count in the cosmic-ray soil moisture observing system. *Journal of Hydrometeorology*, *14*(5), 1659–1671. https://doi.org/10.1175/JHM-D-12-0120.1

Russo, S., Sillmann, J., & Fischer, E. M. (2015). Top ten European heatwaves since 1950 and their occurrence in the coming decades. *Environmental Research Letters*, *10*(12), 124003. https://doi.org/10.1088/1748-9326/10/12/124003

Samaniego, L., Thober, S., Kumar, R., Wanders, N., Rakovec, O., Pan, M., et al. (2018). Anthropogenic warming exacerbates European soil moisture droughts. *Nature Climate Change*, *8*(5), 421–426. https://doi.org/10.1038/s41558-018-0138-5

Santanello, J. A., Dirmeyer, P. A., Ferguson, C. R., Findell, K. L., Tawfik, A. B., Berg, A., et al. (2018). Land-atmosphere interactions: The LoCo perspective. *Bulletin of the American Meteorological Society*, *99*, 1253–1272. https://doi.org/10.1175/BAMS-D-17-0001.1

Santanello, J. A., Friedl, M. A., & Ek, M. B. (2007). Convective planetary boundary layer interactions with the land surface at diurnal time scales: Diagnostics and feedbacks. *Journal of Hydrometeorology*, *8*(5), 1082–1097. https://doi.org/10.1175/JHM614.1

Santanello, J. A., Peters-Lidard, C. D., & Kumar, S. V. (2011). Diagnosing the sensitivity of local land–atmosphere coupling via the soil moisture–boundary layer interaction. *Journal of Hydrometeorology*, *12*(5), 766–786. https://doi.org/10.1175/JHM-D-10-05014.1

Schumacher, D. L., Keune, J., Heerwaarden, C. C. van, Arellano, J. V.-G. de, Teuling, A. J., & Miralles, D. G. (2019). Amplification of mega-heatwaves through heat torrents fuelled by upwind drought. *Nature Geoscience*, *12*(9), 712–717. https://doi.org/10.1038/s41561-019-0431-6

Schwingshackl, C., Hirschi, M., & Seneviratne, S. I. (2018). A theoretical approach to assess soil moisture–climate coupling across CMIP5 and GLACE-CMIP5 experiments. *Earth System Dynamics*, *9*(4), 1217–1234. https://doi.org/10.5194/esd-9-1217-2018

Seneviratne, S. I., Corti, T., Davin, E. L., Hirschi, M., Jaeger, E. B., Lehner, I., et al. (2010). Investigating soil moisture–climate interactions in a changing climate: A review. *Earth-Science Reviews*, *99*(3), 125–161. https://doi.org/10.1016/j.earscirev.2010.02.004

Seneviratne, S. I., Lüthi, D., Litschi, M., & Schär, C. (2006). Land–atmosphere coupling and climate change in Europe. *Nature*, *443*(7108), 205–209. https://doi.org/10.1038/nature05095

Stanley, S., Antoniou, V., Ball, L. A., Bennett, E. S., Blake, J. R., Boorman, D. B., et al. (2019). *Daily and sub-daily hydrometeorological and soil data (2013-2017) [COSMOS-UK]*. Retrieved from https://catalogue.ceh.ac.uk/id/a6012796-291c-4fd6-a7ef-6f6ed0a6cfa5

Teuling, A. J. (2018). A hot future for European droughts. *Nature Climate Change*, *8*(5), 364–365. https://doi.org/10.1038/s41558-018-0154-5

Vautard, R., Yiou, P., D'Andrea, F., de Noblet, N., Viovy, N., Cassou, C., et al. (2007). Summertime European heat and drought waves induced by wintertime Mediterranean rainfall deficit. *Geophysical Research Letters*, *34*(7), L07711. https://doi.org/10.1029/2006GL028001

Vicente-Serrano, S. M., Lopez-Moreno, J.-I., Beguería, S., Lorenzo-Lacruz, J., Sanchez-Lorenzo, A., García-Ruiz, J. M., et al. (2014). Evidence of increasing drought severity caused by temperature rise in southern Europe. *Environmental Research Letters*, *9*(4), 044001. https://doi.org/10.1088/1748-9326/9/4/044001

Wehrli, K., Hauser, M., & Seneviratne, S. I. (2020). *Storylines of the 2018 Northern Hemisphere heat wave at pre-industrial and higher global warming levels*. 22nd EGU General Assembly, Earth System Dynamics Discussions, 1–25. https://doi.org/10.5194/esd-2019-91

Wu, J., & Dirmeyer, P. A. (2020). Drought demise attribution over CONUS. *Journal of Geophysical Research: Atmospheres*, *125*(4), e2019JD031255. https://doi.org/10.1029/2019JD031255

Yiou, P., Cattiaux, J., Faranda, D., Kadygrov, N., Jézéquel, A., Naveau, P., et al. (2020). Analyses of the Northern European Summer Heatwave of 2018. *Bulletin of the American Meteorological Society*, *101*(1), S35–S40. https://doi.org/10.1175/BAMS-D-19-0170.1

Zhang, Y., Wang, L., Santanello, J. A., Pan, Z., Gao, Z., & Li, D. (2020). Aircraft observed diurnal variations of the planetary boundary layer under heat waves. *Atmospheric Research*, *235*, 104801. https://doi.org/10.1016/j.atmosres.2019.104801

Zscheischler, J., Orth, R., & Seneviratne, S. I. (2015). A submonthly database for detecting changes in vegetation-atmosphere coupling. *Geophysical Research Letters*, *42*(22), 9816–9824. https://doi.org/10.1002/2015GL066563

Zscheischler, J., Westra, S., Hurk, B. J. J. M. van den, Seneviratne, S. I., Ward, P. J., Pitman, A., et al. (2018). Future climate risk from compound events. *Nature Climate Change*, *8*(6), 469–477. https://doi.org/10.1038/s41558-018-0156-3